

Photoelectrocatalyzed undirected C–H trifluoromethylation of arenes: catalyst evaluation and scope†

Julia Struwe and Lutz Ackermann  *

Received 10th April 2023, Accepted 5th June 2023

DOI: 10.1039/d3fd00076a

During the last few years, photoelectrocatalysis has evolved as an increasingly viable tool for molecular synthesis. Despite several recent reports on the undirected C–H functionalization of arenes, thus far, a detailed comparison of different catalysts is still missing. To address this, more than a dozen different mediators were employed in the trifluoromethylation of (hetero-)arenes to compare them in their efficacies.

Introduction

Electrochemical synthesis has emerged as a powerful approach in molecular syntheses.¹ Strategies to replace the stoichiometric oxidant through the hydrogen evolution reaction and to enable novel reactivities have gained significant attention.² Likewise, visible-light photoredox catalysis has been recognized as a valuable strategy to allow chemical transformations under mild conditions,³ particularly with efficient single electron transfer (SET).

The merger of electrocatalysis and photochemistry with pioneering work in the 1970s and 1980s⁴ has the power to allow chemistry at extreme potentials⁵ and enabled a diverse set of desirable transformations, such as oxidative C–C,⁶ C–N⁷ and C–O⁸ bond formations through radical mechanisms. In addition, reductive and isohypsic, thus redox-neutral, reactions have also been achieved under photoelectrocatalysis.^{5a} While different photoelectrocatalysts have been employed (Fig. 1a), to the best of our knowledge, a systematic comparison of different photocatalysts has thus far proven elusive.

Thus, given the diversity of different photo- and redox-catalysts, from which some have also been employed in photoelectrocatalyzed reactions, we wished to elucidate the impact of the nature of the photoelectrocatalyst on the reaction efficacies. As a representative testing ground, we selected the photoelectrochemical C–H

Institut für Organische und Biomolekulare Chemie, Georg-August-Universität Göttingen, Tammannstrasse 2, 37077 Göttingen, Germany. E-mail: Lutz.Ackermann@chemie.uni-goettingen.de

† Electronic supplementary information (ESI) available. See DOI: <https://doi.org/10.1039/d3fd00076a>



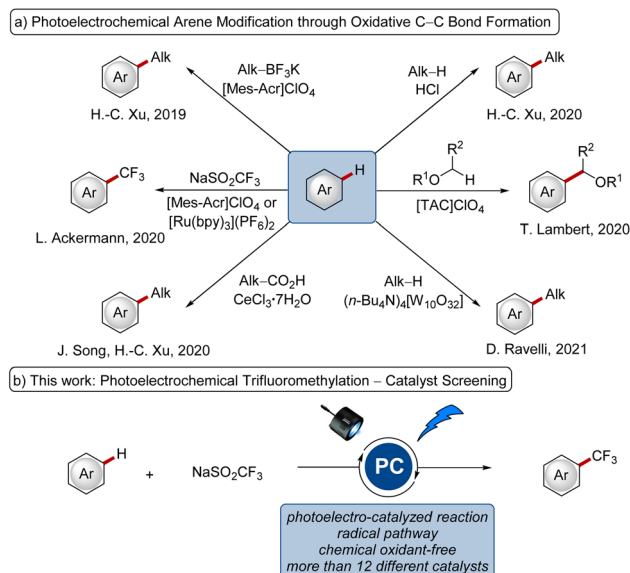


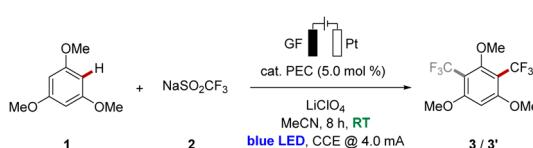
Fig. 1 (a) Overview of photoelectrochemical C–C bond formations and the employed photocatalysts; (b) performance study of different mediators in the photoelectrocatalyzed trifluoromethylation of arenes.

trifluoromethylation of arenes (Fig. 1b)⁹ with the Langlois reagent (**2**, NaSO_2CF_3)¹⁰ as the trifluoromethyl source.

Results and discussion

We commenced our study by testing various photoredox catalysts with 5.0 mol% catalyst loading using 1,3,5-trimethoxybenzene (**1**) as the model substrate, while transition metal-based catalysts were employed at 2.0 mol% (Table 1). The frequently used ruthenium(II) trisbipyridine photocatalyst provided the desired functionalized arene in an excellent conversion yield of 91% (Table 1, entry 1). Additionally, other transition metal catalysts have been explored, and to our delight, the earth-abundant iron- and nickel-derivatives of the trisbipyridine ruthenium(II) catalyst gave comparably good results under otherwise identical reaction conditions (entries 2 and 3). Also, the photocatalyst $(n\text{-Bu}_4\text{N})_4\text{[W}_{10}\text{O}_{32}\text{]}$ enabled good reactivity, although slightly diminished yields of the decorated arenes **3** and **3'** were obtained (entry 4). Cerium trichloride was also able to catalyze the reaction with comparable conversions, with irradiation at 450 nm or 390 nm wavelength (entries 5 and 6). Furthermore, halide salts were suitable mediators, with strongly enhanced reactivities under light irradiation compared to solely electrochemical conditions,¹¹ and the products **3** and **3'** were obtained in yields up to 97% with significant amounts of difunctionalized product **3'** (entries 7–9). Also, other organic photoelectrocatalysts were identified as more sustainable alternatives to the metal-containing ones, furnishing the desired products **3** and **3'** in excellent yields of around 90% (entries 10–14). To our delight, the trisaminocyclopropenium-based catalyst $[\text{TAC}]\text{ClO}_4$ provided the highest mono-



Table 1 Functionalization of trimethoxybenzene **1** with different catalysts^a

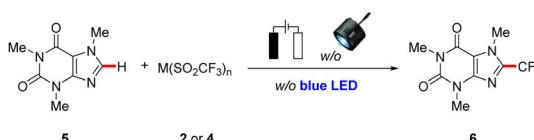
Entry	PEC	Deviation	Conversion (3 : 3')
1	[Ru(bpy) ₃](PF ₆) ₂	2 mol%	91% (3.3 : 1)
2	[Fe(bpy) ₃](PF ₆) ₂	2 mol%	87% (3.8 : 1)
3	[Ni(bpy) ₃]Br ₂	2 mol%	89% (5.2 : 1)
4	(n-Bu ₄ N) ₄ [W ₁₀ O ₃₂] ²⁻	2 mol%	85% (5.5 : 1)
5	CeCl ₃ ·7H ₂ O	—	90% (3.5 : 1)
6	CeCl ₃ ·7H ₂ O	390 nm	93% (2.6 : 1)
7	TBAI	—	95% (2.2 : 1)
8	TBABr	—	97% (1.5 : 1)
9	TBACl	—	95% (1.4 : 1)
10	DCA	—	96% (5.0 : 1)
11	DCN	—	90% (4.3 : 1)
12	DDQ	—	93% (1.7 : 1)
13	[TAC]ClO ₄	—	89% (6.4 : 1)
14	[Mes-Acr]ClO ₄	—	95% (4.9 : 1)
15	[Mes-Acr]ClO ₄	Zn(SO ₂ CF ₃) ₂ (4)	63% (20 : 1)
16	—	—	9% (—)
17	[Mes-Acr]ClO ₄	Without light	7% (—)
18	[Mes-Acr]ClO ₄	Without current	4% (—)

^a Reaction conditions: undivided cell, GF anode (10 mm × 15 mm × 6 mm), Pt cathode (10 mm × 15 mm × 0.25 mm), constant-current electrolysis at 4.0 mA. **1** (0.25 mmol), NaSO₂CF₃ (2, 0.50 mmol) or Zn(SO₂CF₃)₂ (4, 0.25 mmol), PEC (5.0 mol%), LiClO₄ (0.1 M), MeCN (4.0 mL), 30–35 °C, 8 h, under N₂, blue LEDs (450 nm); conversions were determined by ¹H-NMR using dimethyl-terephthalate as an internal standard. The ratio is given as (mono : di) selectivity. GF = graphite felt, PEC = photoelectrocatalyst, LED = light-emitting diode, bpy = 2,2'-bipyridine, TBA = tetra-n-butyl ammonium, DCA = 9,10-dicyanoanthracene, DCN = 1,4-dicyanonaphthalene, DDQ = 2,3-dichloro-5,6-dicyano-1,4-benzoquinone, TAC = trisaminocyclopropenium, Mes-Acr = 9-mesityl-10-methylacridinium.

selectivity for the functionalization, while DDQ resulted in an optimal difunctionalization of substrate **1** (entries 12 and 13). In addition, the sulfinate Zn(SO₂CF₃)₂ (4) could be also employed as the trifluoromethyl source under photoelectrocatalytic conditions, albeit with a significantly diminished conversion (entry 15). In sharp contrast, the reaction failed to proceed in the absence of a photocatalyst (entry 16), thereby reflecting the key influence of the catalytic mediator. Likewise, the essential role of visible light as well as an electric current was verified in control experiments (entries 17 and 18).

Moreover, the impact of the irradiation with visible light was analyzed by comparing the photoelectrocatalytic approach to electrooxidative trifluoromethylations¹² (Table 2). With the user-friendly undivided cell set-up for the electrooxidative transformation, the functionalized arene **6** was obtained at a low conversion of only 21% (Table 2, entry 1). In sharp contrast, the photoelectrocatalysis was found to be uniquely powerful in furnishing arene **6** (Table 2, entry 2).¹¹



Table 2 Electrooxidation vs. photoelectrocatalysis^a

Entry	Sulfinate	Conditions	Yield (6)
1	$Zn(SO_2CF_3)_2$	Electrooxidation	(26%)
2	$Zn(SO_2CF_3)_2$	Photoelectrocatalysis	(80%)
3	$NaSO_2CF_3$	Electrooxidation	(21%)
4	$NaSO_2CF_3$	Photoelectrocatalysis	70% (81%)

^a Reaction conditions: electrooxidation: undivided cell, GF anode (10 mm × 15 mm × 6 mm), GF cathode (10 mm × 15 mm × 6 mm), constant-current electrolysis at 4.0 mA. 5 (0.25 mmol), 2 (0.5 mmol), n -Bu₄NClO₄ (0.15 M), DMSO (5.0 mL), 8 h. Photoelectrocatalysis: undivided cell, GF anode (10 mm × 15 mm × 6 mm), Pt cathode (10 mm × 15 mm × 0.25 mm), constant-current electrolysis at 4.0 mA. 5 (0.25 mmol), 2 (0.5 mmol), [Mes-Acr]ClO₄ (5.0 mol%), LiClO₄ (0.1 M), MeCN (4.0 mL), 30–35 °C, 8 h, under N₂, blue LEDs (450 nm). Yields refer to the isolated product, conversions were determined by ¹⁹F-NMR using 1-fluorononane as internal standard.

Further studies on the efficiency of the different catalysts were performed through the analysis of the reaction mixture in a time-resolved manner. Caffeine (5) was chosen as the model substrate to avoid any difficulties in interpretation because of difunctionalization (Fig. 2). A comparison of the data showed only minor differences during the reaction process. However, slight differences in the catalytic performance of the catalysts were reflected in the product yields, which differ by around 15% after 8 h reaction time, with the best results for DCN and TBACl. The determined faradaic efficiency of this undirected C–H functionalization ranged from 40% to 47% with a current density of 1/400 A cm^{−2}.

The undirected C–H functionalization with the Langlois reagent was proposed as shown in Scheme 1.⁹ In the case of the organic dye [Mes-Acr]ClO₄, the SET was enabled by the excited-state photocatalyst species, which was generated after absorption of blue light, resulting in the formation of a trifluoromethyl radical after fragmentation. Likewise, the reduced photocatalyst was formed and subsequently reoxidized at the anode. Subsequent modification of the arenes follows a radical pathway with a Wheland complex as the key intermediate.

With a set of viable photoredox catalysts for the undirected C–H trifluoromethylation of arenes in hand, we became interested in further substantiating the catalytic performance of representative photoelectrocatalysts with a series of arenes 7 (Scheme 2 top). Besides triethylbenzene, several heterocyclic systems were tested, among those quinolines and pyrimidine derivatives. These examples of nitrogen containing heterocycles furnished the corresponding products 10–12 in moderate to good yields being similar for both catalysts. Furthermore, furane as well as thiophene scaffolds were fully tolerated in both catalytic systems to access 13–15, although the decorated heterocyclic amides 14 and 15 were obtained as a mixture of two regioisomers. Moreover, several heterocyclic compounds associated with natural products were employed as well.



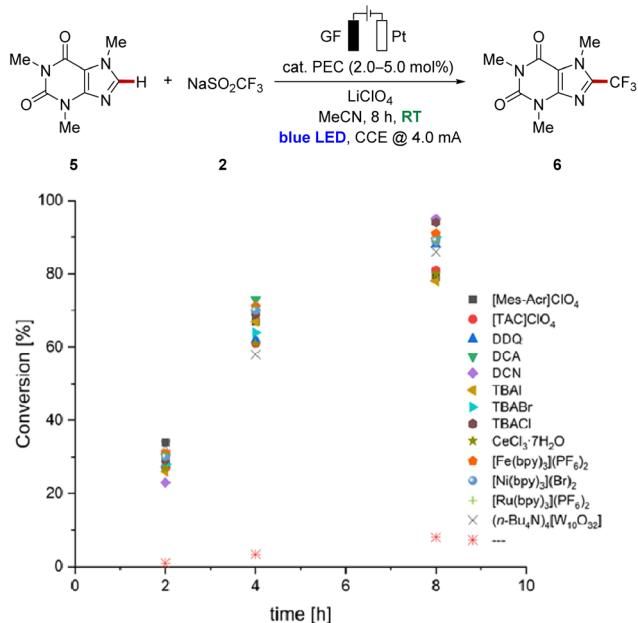
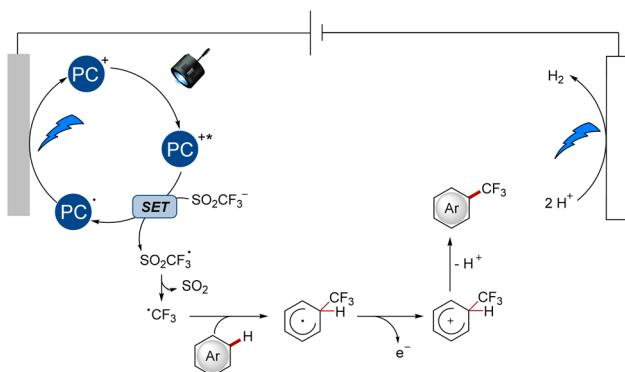


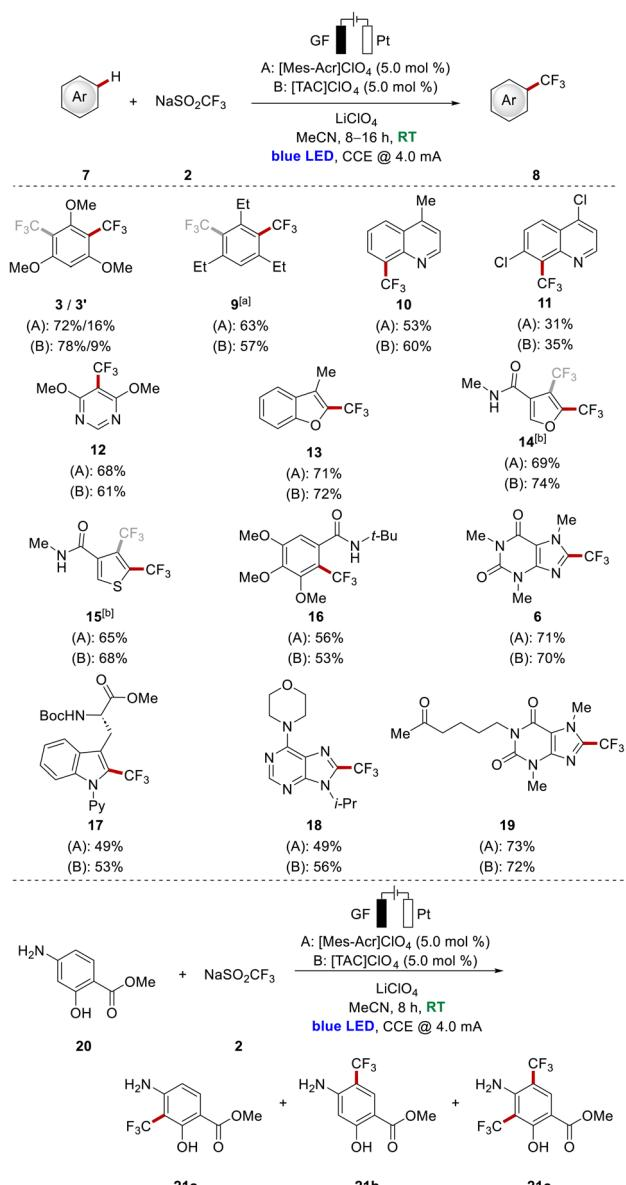
Fig. 2 Comparison of different catalysts for the trifluoromethylation of caffeine (5). Reaction conditions: undivided cell, GF anode (10 mm × 15 mm × 6 mm), Pt cathode (10 mm × 15 mm × 0.25 mm), constant-current electrolysis at 4.0 mA, 5 (0.30 mmol), 2 (0.60 mmol), catalyst (2.0 mol% or 5.0 mol%), LiClO₄ (0.1 M), MeCN (4.0 mL), 30–35 °C, 8 h, under N₂, blue LEDs (450 nm). Conversions were determined after 2, 4 and 8 hours by ¹⁹F-NMR using 1-fluorononane as an internal standard.



Scheme 1 Proposed catalytic cycle for the undirected functionalization with [Mes-Acr]ClO₄ as the photocatalyst.

Among those, a gallic acid derivative, pentoxyfylline as well as a purine base and modified tryptophan were smoothly converted into the corresponding products **16–19** with moderate to good yields. For all the depicted examples, the isolated yield was comparable for both catalysts, with differences of up to 7%.

Interestingly, in the case of arene **20**, which is a building block in the synthesis of the anti-cancer kinase inhibitor KAN0438757,¹³ the reaction outcome was



Scheme 2 Comparison of [Mes-Acr]ClO₄ and [TAC]ClO₄ for different arenes. Reaction conditions: undivided cell, GF anode (10 mm × 15 mm × 6 mm), Pt cathode (10 mm × 15 mm × 0.25 mm), 7 (0.25 mmol), 2 (0.50 mmol), [Mes-Acr]ClO₄ or [TAC]ClO₄ (5.0 mol %), LiClO₄ (0.1 M), MeCN (4.0 mL), 30–35 °C, 8–16 h, under N₂, blue LEDs (450 nm); isolated yields. ^aProduct was obtained together with the difunctionalized product. ^bProduct was obtained as a mixture of regioisomers. ^cReaction conditions: undivided cell, GF anode (10 mm × 15 mm × 6 mm), Pt cathode (10 mm × 15 mm × 0.25 mm), constant-current electrolysis at 4.0 mA, 20 (0.25 mmol), 2 (0.50 mmol), [Mes-Acr]ClO₄ or [TAC]ClO₄ (5.0 mol %), LiClO₄ (0.1 M), MeCN (4.0 mL), 30–35 °C, 8 h, under N₂, blue LEDs (450 nm); isolated yields.

significantly influenced by the choice of the catalyst in terms of the yield and the ratio of the obtained products **21a–c** (Scheme 2, bottom). For this substrate, possessing sensitive free hydroxyl- and amine functionalities, $[\text{TAC}]\text{ClO}_4$ outperformed $[\text{Mes-Acr}]\text{ClO}_4$ with an isolated total product yield of 76%. Thus, the result indicates the potential of $[\text{TAC}]\text{ClO}_4$ for the functionalization of sensitive substrates.

Conclusions

In conclusion, we reported on an evaluation of various photoelectrocatalysts for the undirected C–H trifluoromethylation of arenes. Thereby, we identified two powerful metal-free photoelectrocatalysts, $[\text{Mes-Acr}]\text{ClO}_4$ and $[\text{TAC}]\text{ClO}_4$, for direct C–H trifluoromethylation without directing groups, enabling efficient photoelectrocatalysis under mild conditions with ample scope. However, the exact mode of action of the catalyst might differ between different catalysts, dependent on the properties.

Conflicts of interest

There are no conflicts to declare.

Acknowledgements

Generous support by DZHK and the DFG (Gottfried Wilhelm Leibniz prize to L. A.) is gratefully acknowledged.

References

- 1 (a) M. C. Leech and K. Lam, *Nat. Rev. Chem.*, 2022, **6**, 275–286; (b) N. Chen and H.-C. Xu, *Chem. Rec.*, 2021, **21**, 2306–2319; (c) L. F. T. Novaes, J. Liu, Y. Shen, L. Lu, J. M. Meinhardt and S. Lin, *Chem. Soc. Rev.*, 2021, **50**, 7941–8002; (d) C. Zhu, N. W. J. Ang, T. H. Meyer, Y. Qiu and L. Ackermann, *ACS Cent. Sci.*, 2021, **7**, 415–431; (e) F. Wang and S. S. Stahl, *Acc. Chem. Res.*, 2020, **53**, 561–574; (f) W. R. Browne, *Electrochemistry*, Oxford Chemistry Press, Oxford, 2019; (g) M. Elsherbini and T. Wirth, *Acc. Chem. Res.*, 2019, **52**, 3287–3296; (h) A. Scheremetjew, T. H. Meyer, Z. Lin, L. Massignan and L. Ackermann, in *Science of Synthesis: Electrochemistry in Organic Synthesis*, ed. L. Ackermann, Thieme, Stuttgart, 2019, pp. 3–32; (i) A. Wiebe, T. Gieshoff, S. Möhle, E. Rodrigo, M. Zirbes and S. R. Waldvogel, *Angew. Chem., Int. Ed.*, 2018, **57**, 5594–5619; (j) M. Yan, Y. Kawamata and P. S. Baran, *Chem. Rev.*, 2017, **117**, 13230–13319; (k) R. Francke and R. D. Little, *Chem. Soc. Rev.*, 2014, **43**, 2492–2521.
- 2 (a) C.-Y. Cai, Z.-J. Wu, J.-Y. Liu, M. Chen, J. Song and H.-C. Xu, *Nat. Commun.*, 2021, **12**, 3745; (b) M. Hielscher, E. K. Oehl, B. Gleede, J. Buchholz and S. R. Waldvogel, *ChemElectroChem*, 2021, **8**, 3904–3910; (c) M. Stangier, A. M. Messinis, J. C. A. Oliveira, H. Yu and L. Ackermann, *Nat. Commun.*, 2021, **12**, 4736; (d) H.-J. Zhang, L. Chen, M. S. Oderinde, J. T. Edwards, Y. Kawamata and P. S. Baran, *Angew. Chem., Int. Ed.*, 2021, **60**, 20700–20705; (e) F. Xu, H. Long, J. Song and H.-C. Xu, *Angew. Chem., Int. Ed.*, 2019, **58**,



9017–9021; (f) N. Sauermann, T. H. Meyer, C. Tian and L. Ackermann, *J. Am. Chem. Soc.*, 2017, **139**, 18452–18455; (g) E. J. Horn, B. R. Rosen, Y. Chen, J. Tang, K. Chen, M. D. Eastgate and P. S. Baran, *Nature*, 2016, **533**, 77–81.

3 (a) A. Y. Chan, I. B. Perry, N. B. Bissonnette, B. F. Buksh, G. A. Edwards, L. I. Frye, O. L. Garry, M. N. Lavagnino, B. X. Li, Y. Liang, E. Mao, A. Millet, J. V. Oakley, N. L. Reed, H. A. Sakai, C. P. Seath and D. W. C. MacMillan, *Chem. Rev.*, 2022, **122**, 1485–1542; (b) N. A. Romero and D. A. Nicewicz, *Chem. Rev.*, 2016, **116**, 10075–10166; (c) J. M. R. Narayanan and C. R. J. Stephenson, *Chem. Soc. Rev.*, 2011, **40**, 102–113.

4 (a) R. Scheffold and R. Orlinski, *J. Am. Chem. Soc.*, 1983, **105**, 7200–7202; (b) J.-C. Moutet and G. Reverdy, *J. Chem. Soc., Chem. Commun.*, 1982, 654–655; (c) J.-C. Moutet and G. Reverdy, *Tetrahedron Lett.*, 1979, **20**, 2389–2392.

5 (a) H. Huang, K. A. Steiniger and T. H. Lambert, *J. Am. Chem. Soc.*, 2022, **144**, 12567–12583; (b) J. P. Barham and B. König, *Angew. Chem., Int. Ed.*, 2020, **59**, 11732–11747; (c) J. Galczynski, H. Huang and T. H. Lambert, in *Science of Synthesis: Electrochemistry in Organic Synthesis*, ed. L. Ackermann, Thieme, Stuttgart, 2019, pp. 325–362.

6 (a) C.-Y. Cai, X.-L. Lai, Y. Wang, H.-H. Hu, J. Song, Y. Yang, C. Wang and H.-C. Xu, *Nat. Catal.*, 2022, **5**, 943–951; (b) L. Capaldo, L. L. Quadri, D. Merli and D. Ravelli, *Chem. Commun.*, 2021, **57**, 4424–4427; (c) H. Huang, Z. M. Strater and T. H. Lambert, *J. Am. Chem. Soc.*, 2020, **142**, 1698–1703; (d) X.-L. Lai, X.-M. Shu, J. Song and H.-C. Xu, *Angew. Chem., Int. Ed.*, 2020, **59**, 10626–10632; (e) P. Xu, P.-Y. Chen and H.-C. Xu, *Angew. Chem., Int. Ed.*, 2020, **59**, 14275–14280; (f) H. Yan, Z.-W. Hou and H.-C. Xu, *Angew. Chem., Int. Ed.*, 2019, **58**, 4592–4595.

7 (a) T. Shen and T. H. Lambert, *Science*, 2021, **371**, 620–626; (b) T. Shen and T. H. Lambert, *J. Am. Chem. Soc.*, 2021, **143**, 8597–8602; (c) L. Niu, C. Jiang, Y. Liang, D. Liu, F. Bu, R. Shi, H. Chen, A. D. Chowdhury and A. Lei, *J. Am. Chem. Soc.*, 2020, **142**, 17693–17702; (d) H. Huang, Z. M. Strater, M. Rauch, J. Shee, T. J. Sisto, C. Nuckolls and T. H. Lambert, *Angew. Chem., Int. Ed.*, 2019, **58**, 13318–13322; (e) F. Wang and S. S. Stahl, *Angew. Chem., Int. Ed.*, 2019, **58**, 6385–6390; (f) L. Zhang, L. Liardet, J. Luo, D. Ren, M. Grätzel and X. Hu, *Nat. Catal.*, 2019, **2**, 366–373.

8 (a) H. Huang and T. H. Lambert, *Angew. Chem., Int. Ed.*, 2021, **60**, 11163–11167; (b) H. Huang and T. H. Lambert, *J. Am. Chem. Soc.*, 2021, **143**, 7247–7252.

9 Y. Qiu, A. Scheremetjew, L. H. Finger and L. Ackermann, *Chem.-Eur. J.*, 2020, **26**, 3241–3246.

10 (a) J. Shen, J. Xu, L. He, C. Liang and W. Li, *Chin. Chem. Lett.*, 2022, **33**, 1227–1235; (b) Y. Ji, T. Brueckl, R. D. Baxter, Y. Fujiwara, I. B. Seiple, S. Su, D. G. Blackmond and P. S. Baran, *Proc. Natl. Acad. Sci. U. S. A.*, 2011, **108**, 14411–14415; (c) B. R. Langlois, E. Laurent and N. Roidot, *Tetrahedron Lett.*, 1991, **32**, 7525–7528.

11 For detailed information, see the ESI†

12 A. G. O'Brien, A. Maruyama, Y. Inokuma, M. Fujita, P. S. Baran and D. G. Blackmond, *Angew. Chem., Int. Ed.*, 2014, **53**, 11868–11871.

13 N. M. S. Gustafsson, K. Färnegårdh, N. Bonagas, A. H. Ninou, P. Groth, E. Wiita, M. Jönsson, K. Hallberg, J. Lehto, R. Pennisi, J. Martinsson, C. Norström, J. Hollers, J. Schultz, M. Andersson, N. Markova, P. Marttila, B. Kim, M. Norin, T. Olin and T. Helleday, *Nat. Commun.*, 2018, **9**, 3872.

